Progress In Electromagnetics Research C, Vol. 44, 27–40, 2013

AN ALTERNATIVE TECHNIQUE FOR ESTIMATING THE K-FACTOR FROM THE PHASE OF THE ELECTROMAGNETIC FIELD WITHIN A REVERBERATING CHAMBER

Antonio Sorrentino*, Giuseppe Ferrara, Angelo Gifuni, and Maurizio Migliaccio

Dipartimento di Ingegneria, Università degli Studi di Napoli Parthenope, Centro Direzionale, Isola C4, Napoli 80143, Italy

Abstract—In this paper, an alternative technique for estimating the Rice factor, K, is applied to the phase of electromagnetic field within a reverberating chamber (RC) for classifying the fading depth on the coherent components in the emulated line-of-sight (LOS) environments. The estimator is time-effective and general, and can be applied for any angle of arrival (AoA) of the received field and for any time varying propagation channel as a complementary method to the classical estimators for evaluating K above all when small but consistent coherent components are present. Measurements accomplished at the RC of the Università di Napoli Parthenope (formerly Istituto Universitario Navale, IUN) confirm the goodness of the proposed technique.

1. INTRODUCTION

With the growing use of wireless devices in daily life there is an increasing need for a test site that is able to emulate different environments where such devices are used. For its characteristics, the Reverberating Chamber (RC) enjoys growing popularity as an emulator of real life environments [1–3]. The RC is an electrically large, metallic enclosure in which the input electromagnetic field is randomized by means of appropriately tailored processes [4, 5]. Usually, large metallic paddles, called stirrers, are moved inside the chamber enabling to change the boundary conditions within the RC. This fact gives rise to a chaotic process [6] that provides a stochastic

Received 2 August 2013, Accepted 11 September 2013, Scheduled 13 September 2013
* Corresponding author: Antonio Sorrentino (antonio.sorrentino@uniparthenope.it).

field, isotropic and uniform. Essentially, the stochastic model within the RC can be described by means of the Rice model that can be expressed by the Rice factor, K, i.e.,

$$K = \frac{\left|\hat{E}\right|^2}{2\sigma^2} \tag{1}$$

where $|\hat{E}|^2$ is the power of the coherent component and $2\sigma^2$ the power of the incoherent component of the field. When K is equal to zero, i.e., no coherent component is present within the chamber, the Rice model becomes a Rayleigh one [7].

The RC has been employed as a test site for several wireless applications which include, but not limited to, antenna measurements [8–12], emulation of line-of-sight (LOS) and no LOS propagation channels [1, 13–18], and multiple input multiple output (MIMO) system performance [19, 20]. In all the above-mentioned applications, the existence of a proper estimation of K plays a key role in the definition of the emulated environments. In order to estimate K from the RC measurements, several methods have been proposed [16, 17, 21–23]. Such methods use the measured power signals — amplitude only, no phase — for a proper K estimation.

Although the K amplitude estimator works well in the channels characterized by an high coherent to incoherent power ratio of the received field, when small but consistent coherent component is present, it can be analytically shown that K amplitude estimator is not finely grained enough to properly discriminate such components [14]. In such cases, a K estimator can be accomplished from the phase of the electromagnetic field. As matter of fact, the Rice phase distribution has been employed to evaluate K [24–26]. In [24] the Rice phase probability density function (pdf) is used to find a maximum likelihood estimator (MLE) of K. However, since the Rice phase pdf is more complicated than the Rice amplitude pdf, an approximate solution exists only when $K \geq 5$. In [25], using polar signals, a complex signal based MLE is proposed. This estimator works well when the Doppler shift is zero but is not robust when the channel is time varying. The K estimator proposed in [26] overcomes the drawbacks of the two previous methods but presents several limitations. First, the estimator does not work for angle of arrival (AoA) of the dominant component perpendicular to the mobile trajectory. Second, the estimator is derived assuming isotropic scattering for the multipath components.

In this paper, based on the phase pdf of the electromagnetic field, a K estimator is proposed. The proposed estimator is first applied to the phase of the received electromagnetic field within a RC that has been employed for the emulation of both isotropic and

non-isotropic environments [27]. It has high performance especially to discriminate small but consistent coherent components. Further, the estimator works well for any time-varying channels and for any AoA of the coherent component, including the angles in which the dominant component is perpendicular to the direction of the transmitting antenna.

Experiments conducted at the RC of the Università degli Studi di Napoli Parthenope (formerly Istituto Universitario Navale, IUN), when the chamber emulates several LOS environments, witness the effectiveness of the proposed methodology that is general and suitable for a large class of signals in which the information of the phase can be used as a complement for the classical K estimation.

2. K ESTIMATION FROM THE PHASE OF THE ELECTROMAGNETIC FIELD

In a RC the electromagnetic field has a circular Gaussian distribution where the real and imaginary parts are usually no zero mean normally distributed. Hence, the amplitude and phase are Rice distributed [14]

$$p(E) = \frac{|E|}{\sigma^2} \exp\left(-\frac{|E|^2}{2\sigma^2}\right) \exp(-K) I_0\left(\frac{|E|}{\sigma}\sqrt{2K}\right) \tag{2}$$

$$p(\varphi) = \frac{1}{2\pi} \exp(-K) \left\{1 + b\sqrt{\pi} \exp\left(b^2\right) [1 + \operatorname{erf}(b)]\right\} \tag{3}$$

where $|E|$ and φ are the amplitude and the phase of the electromagnetic field, and σ is the standard deviation, K the Rice factor, I_0 the first order Bessel function, $\operatorname{erf}(\cdot)$ the error function, and

$$b = \frac{1}{\sigma\sqrt{2}} \left(\hat{E}_r \cos\varphi_m + \hat{E}_i \sin\varphi_m\right). \tag{4}$$

$\hat{E}_r$ and $\hat{E}_i$ are the means of the real and imaginary parts of coherent component of the field, i.e.,

$$\hat{E} = \hat{E}_r + i\hat{E}_i = \left|\hat{E}\right| \exp(i\varphi_m), \tag{5}$$

being $i = \sqrt{-1}$ and φ_m the angle of the coherent component of the field. Note that $\varphi \neq \varphi_m$.

Equation (4) is strictly related to the expression of K; further, since K is given by the coherent to incoherent power ratio of the received field, it is independent from the angle φ_m of the coherent component. This means that for a given condition, K value is always the same, independent from the φ_m value. Hence, if one supposes that

$\varphi_m = 0$, i.e., the imaginary part of the coherent component of the field has zero mean, one finds [14]

$$b = \frac{1}{\sigma\sqrt{2}}\hat{E}_r \cos\varphi = \sqrt{K\cos\varphi}. \tag{6}$$

By substituting (6) in (3), one obtains

$$p(\varphi) = \frac{1}{2\pi}\exp(-K)\left\{1 + \sqrt{K\pi\cos\varphi}\exp\left(K\cos^2\varphi\right)\left[1 + \operatorname{erf}(\sqrt{K}\cos\varphi)\right]\right\} \tag{7}$$

Equation (7) is the phase of the electromagnetic field within an RC expressed in terms of K. If one wants to evaluate K values especially when small but consistent coherent components are present, one can set $\varphi = \frac{\pi}{2}$, that means $\cos(\varphi) = 0$. Hence, (7) is reduced to

$$p(\varphi = \pi/2) = \frac{1}{2\pi}\exp(-K). \tag{8}$$

From (8), it is simple to derive K as follows

$$K = -\left[\ln(2\pi) + \ln\left(p(\varphi = \pi/2)\right)\right] \tag{9}$$

It is important to note that the condition $\varphi = \pi/2$ is the simplest one to evaluate K, and this condition is particularly indicated for discriminating small but consistent coherent component. Such a condition has a drawback that leads to a limitation on the range of estimated Kvalues. In particular, values of $K > 8$ cannot be estimated (see Section 3). In order to generalize the method and to obtain estimations for any K value, a different condition for the φ angle must be chosen.

3. *K* COMPARISON BETWEEN THE POWER AND THE PHASE ESTIMATOR

In this section, a comparison between the theoretical K values and simulated ones from the phase and from the power is presented. It must be noted that the power estimator has been accomplished as in [21], i.e.,

$$\hat{K}_p = \frac{N-1}{N-2} \times \frac{\left|\hat{E}_r^2\right| + \left|\hat{E}_i^2\right|}{2\sigma^2} - \frac{1}{N}, \tag{10}$$

where N is the number of independent samples, and the subscript p states for power.

Figure 1 shows the results of the comparison between the theory (black line) and simulated data. For a fair comparison, the samples used to estimate K are generated by using the same parameter setup. Here, 16×10^3 samples are used to obtain the same number of samples

used in RC measurements. Note that trials with a different number of samples are also accomplished (results are not shown to save space). For the sake of simplicity, the standard deviation used in the current simulation is equal to 1. The blue points are relative to the K estimator from the phase, where the red points are relative to the K estimator from the amplitude. It is important to observe that no interpolation must have done to obtain the value $\varphi = \pi/2$ from the phase pdf since the center of the bin relative to $\pi/2$ corresponds to the same angle. The performance of the two estimators against the theoretical K values is shown in Figure 1, for the range $0 \leq K < 8$. Although the general agreement is overall satisfactory, three different regions can be distinguished. As matter of fact, one can divide K values into three regions.

The first one is the $0 \leq K \leq 2$ region. It can be noted that although both estimators are very close to the theoretical one, the K phase estimator seems to have an error smaller than the K power estimator. In order to confirm such perception, in Figure 2 the root mean square error (RMSE) of the two estimators is shown. The number of simulations used for evaluating the RMSE error is equal to 15. As shown in Figure 2, the RMSE error of the K phase estimator (black dotted line) is smaller than the one for the K power estimator (red dotted line) witnessing that a best estimation is obtained.

The second region is the $2 < K \leq 6$ region. Here, the RMSE

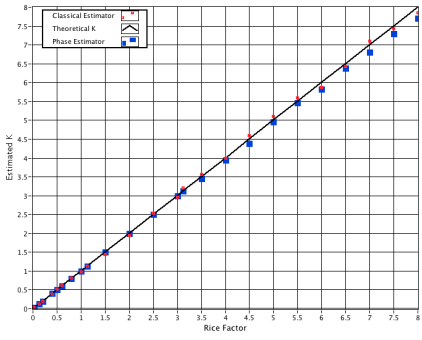

Figure 1. Comparison between the theoretical (continuous line) and the simulated K factors. The simulated values are represented by red circle (phase estimator) and blue square (amplitude estimator).

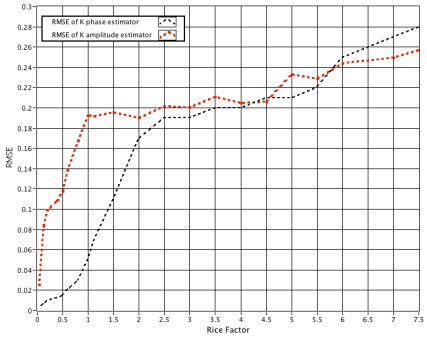

Figure 2. Comparison between the Root Mean Square Error (RMSE) of the phase (black dotted line) and the power (red dotted line) estimators of K.

values of K phase estimators are slightly greater than the ones into the previous region (see Figure 2). As matter of fact, the two RMSE differ so little that the estimators show performance comparable in the K estimation.

The last region is the $6 < K < 8$ region. The performance of the K phase estimator slightly degrades with respect to the previous cases, but it is also comparable to the K amplitude estimator (see Figure 2). According to the theory (see Section 2), the estimation of K cannot be accomplished for $K \geq 8$. Physically, this is due to the phase angle $\varphi = \pi/2$. From statistical analysis, having the electromagnetic field a complex normal distribution, each Gaussian pdf can be considered divided into several σ intervals. The first interval corresponds to 68% of values drawn from a normal distribution, which are within one σ away from the mean. The seconds one accounts for about 95% of the values that lie within 2σ, and the third interval accounts for about 99.7% that are within 3σ [28]. In order to account for the 99.9% of samples, about 4σ must be considered. It is important to note that $\varphi = \pi/2$ is the angle between the real and imaginary axis (see Figure 3). If the coherent part is read in terms of real part, when this last one increases, the scattered plot moves toward the right side with respect to the imaginary axis. $\varphi = \pi/2$ applies if the real part does not become greater than 4σ that can be seen as the radius of the scattered plot (see Figure 4). For values of the coherent component greater than 4σ, the scattered plot is totally over the imaginary line

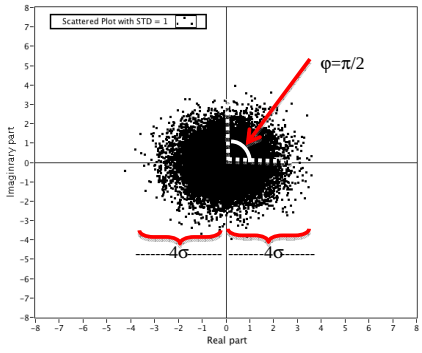

Figure 3. Simulated scattered plot of the electromagnetic field with no coherent component and the φ angle shown. In all the simulations $\sigma = 1$.

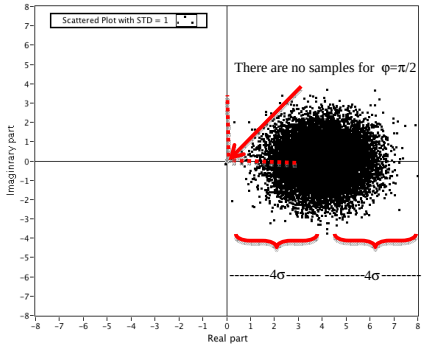

Figure 4. Simulated scattered plot of the electromagnetic field with a coherent component equal to 4. There are no samples at $\varphi = \pi/2$.

(see Figure 4); no samples are at $\varphi = \pi/2$. Hence, the estimation of K cannot be accomplished. In terms of mathematical formulation, called $|\hat{E}|$ the coherent amplitude component of the received field, the limit conditions can be expressed as

$$\left|\hat{E}\right| < 4\sigma \Rightarrow \left|\hat{E}\right|^2 < 16\sigma^2 \tag{11}$$

that in terms of K means

$$\begin{gathered} \left|\hat{E}\right|^2 < 16\sigma^2 \Rightarrow \frac{\left|\hat{E}\right|^2}{8} < 2\sigma^2 \\ \Downarrow \\ \frac{\left|\hat{E}\right|^2}{2\sigma^2} < 8 \Rightarrow K < 8 \end{gathered} \tag{12}$$

With the conditions $\varphi = \pi/2$, (12) says that an estimation of K from the phase cannot be accomplished for values of K equal or greater than 8.

4. EXPERIMENTAL RESULTS

In this section, a meaningful set of experimental results which aim to support the new approach is presented. A simple and very effective technique to estimate K from the phase pdf of the received field is proposed and successfully applied to RC measurements. The data analyzed are collected by making use of the RC located at the IUN. It is a $8\,\mathrm{m}^3$ cubic chamber whose internal walls and stirrers are made of aluminum. Three rotating stirrers are present (Figure 5): the first stirrer (S1) is on the left of the entrance door, and its shape is rectangular of about $1.84\,\mathrm{m} \times 0.45\,\mathrm{m}$ size; the second stirrer (S2) is in front of the entrance door, and its shape is approximately a Greek cross whose bars are about of $1.84\,\mathrm{m} \times 0.25\,\mathrm{m}$ size; the third stirrer (S3) is located on the top of the chamber and is similar to S2 but for bars sizes which are about $1.20\,\mathrm{m} \times 0.18\,\mathrm{m}$. The three stirrers can rotate at 190 rpm, 320 rpm and 390 rpm, respectively. The transmitting and receiving antennas are both ETS-Lindgren double-ridged waveguide horn certified to work in the 1–18 GHz frequency range. The transmitting antenna (T) is close to the left entering wall of the chamber, and the receiving antenna (R) is close to the right entering wall of the chamber, faced to the transmitting antenna, and are about 1 m above the floor. In such a way, the Rice distribution is realized [16]. An Agilent Technologies Vector Network Analyzer (VNA) is used to transmit and to receive monochromatic signals:

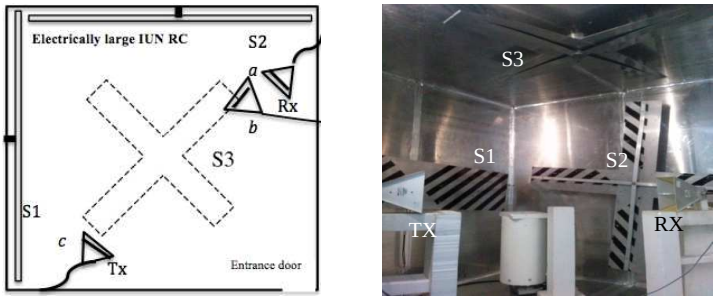

(a) (b)

Figure 5. (a) Schematic top view of the IUN RC. (b) Photo of the inner of the IUN RC.

16001 samples over a 3.6 s period are acquired at a sampling rate of 0.225 ms. The frequency used is equal to 1.8 GHz. A full calibration of the system is *a priori* accomplished. The scattering coefficient S_{21} is measured, and an off-line data analysis is accomplished. The software used for offline analysis of the acquired data is developed in LabVIEW, a graphical development environment of National Instruments. Assuming a distance of 0.30 m from the walls and stirrers, the working volume (WV) one considered exhibits an area of about $2\,\mathrm{m}^2$ and a volume of about $3\,\mathrm{m}^3$ [29]. The shape of the WV well suits for the channel conditions emulated in the RC. Figure 5 shows a sketch of the RC measurement configurations and a photo of the inner of the IUN RC with the three stirrers.

The electromagnetic complex field in the chamber can be seen as two combined contributions. The random one is the results of the mechanical stirring and related to the reflection and diffraction from the RC wall and stirrers. The second one, the deterministic, i.e., the coherent component, is related to the direct link between the transmitting and the receiving antennas within the RC. The direct link is evaluated by making the mean of the real and imaginary parts of the received field. Accordingly, it is a complex value with proper amplitude and phase (see Figure 6). The white line represents the amplitude of the coherent component. The angle φm between the white line and the real axes is its phase. If this angle tends to zero, the scattered plot moves toward the real axes without changing the power ratio between the direct to scattered contributions, i.e., K. Hence, the same K appears in the first scattered plot (grey points) and in the second one (black points) of Figure 6. It must be noted that although K in both the scattered plot has the same value, the proportion of the real and imaginary parts of the coherent component in K estimation

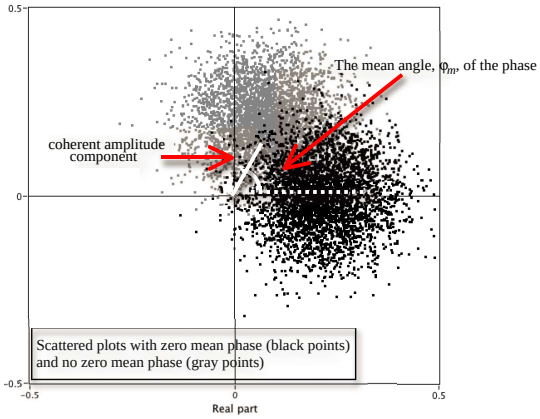

Figure 6. Scattered plot of the RC measurements data with the zero value and no zero value of the imaginary part of the coherent component of the field. The white line is the coherent amplitude component. φ_m is the phase of the coherent component.

is changed. With respect to the black scattered plot, the imaginary part of the coherent component is equal to zero (since the complex electromagnetic field lies on the real axes) while the real part is equal to

$$\hat{E}_r = \sigma\sqrt{2K}. \tag{13}$$

In order to achieve this, the phase φ_m of the coherent component is moved to zero. The φ_m angle is the mean value of the total phase of the electromagnetic field. Hence, $\varphi_m = 0$ means that a zero mean phase must be considered to obtain an electromagnetic field given by an only real coherent part with the same K.

In the first set of experiments, a measurement with the RC unloaded and with the two antennas faced and placed about 1 m far from each other is accomplished. In such a situation, a LOS condition is realized. Following the rationale above explained, a zero mean phase has been evaluated from the received samples. The transmitting antenna is in c position while the receiving one is in a (see Figure 5). The mean of the phase has been evaluated and subtracted to the total phase of the electromagnetic field. Figure 7 shows the phase pdf of the received samples with (dotted line) and without (continuous line) the mean values for the first set of experiments. As one can note, the shape of the phase shown in Figure 7 is the same. According to (9), K is evaluated by considering the value of the zero mean phase in $\pi/2$. The relative K value is equal to 0.461. K values are listed in

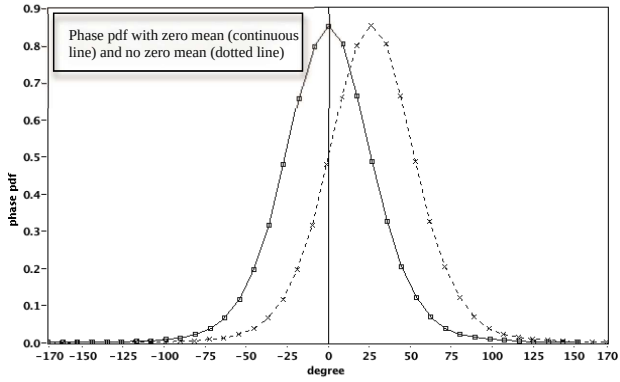

Figure 7. Phase of the received field with (dotted line) and without (continuous line) φ_m.

Table 1. K values from RC measurements.

RC Configuration	***K* phase estimator**
1 meter between Tx and Rx antennas	0.461
0.90 m meter between Tx and Rx antennas	0.560
0.80 m meter between Tx and Rx antennas	0.630
1 absorber within IUN RC	1.360
2 absorber within IUN RC	1.895
3 absorber within IUN RC	2.440
4 absorber within IUN RC	3.917
5 absorber within IUN RC	5.062
6 absorber within IUN RC	6.129
7 absorber within IUN RC	7.432
0.80 m meter between Tx and Rx antennas with Rx antenna perpendicular to Tx one	0.062

Table 1. In [17], it has been shown that the K values are function of the distance between the antennas, if the chamber characteristics remain constant. In order to increase K in the emulated channels, antennas are placed at a smaller distance from each other than the previous cases. Experiments, with a distance of about 0.90 m and about 0.80 m between the two antennas, are accomplished. Hence, the zero mean

phase and K are evaluated. As matter of fact, K is equal to 0.560 and 0.630 at a 0.90 and 0.80 m, respectively. To further increase K values, additional experiments are accomplished with decreasing the Q of the RC by placing an increasing number of absorber in the chamber. The absorbers used in all experiments are C-RAM SFC-24 of the Cuming Corporation, and they are squared base prisms of 0.22 m of height and 0.13 m of base side. The absorbers are placed on polystyrene supports at different heights above the floor without interfering with the coherent component between the two antennas. The values of K estimator from the phase of the received field are listed in Table 1. Finally, a situation with the coherent component perpendicular to the receiving antenna is accomplished (see Figure 5). The transmitting antenna is placed in c position while the receiving antenna is placed in b. The relative position of the transmitting antenna is normal to the position of the receiving one, that is the case in which a dominant, i.e., coherent component is perpendicular to the mobile trajectory. The K value obtained in this case is equal to 0.062. K values greater than 8 are not reported in Table 1. It is important to observe that this work is concerned to the estimation of K values especially when small but consistent coherent components are present in the received field. In general, (7) can be employed for any K, also for $K > 8$, simply changing the condition expressed by $\cos(\varphi) = 0$, i.e., $\varphi = \pi/2$. The chosen condition is the simplest one in order to derive a simple K formula given by (9). A different choice of φ value can also be accomplished in order to derive a general and time-effective formula for any K values.

In summary, an alternative method for the K estimation from the phase of the electromagnetic field has been provided. A K phase estimator has been accomplished and successfully tested on the RC data. The K estimator has high performance for values smaller than 2 while, for the chosen conditions, values greater than 8 cannot be estimated.

5. CONCLUSIONS

In this paper, a K estimator from the phase of the electromagnetic field has been presented and successfully employed on the IUN RC measurements. The K phase estimator has great performance for any time varying channels. Further, it works well for the case in which a dominant component is perpendicular to the mobile trajectory. With respect to the classical power estimator, the proposed estimator shows high performance especially for situations in which small but consistent coherent components are present, i.e., $K < 2$. The condition employed

to derive the K estimator, i.e., $\varphi = \pi/2$, is the simplest one, but it leads to a limitation in the K estimation. The limitation can be easily overcome, and the technique can be used for any K values by choosing a different φ value. The estimator is really simple, robust and general, i.e., suitable to a large class of signal as a complementary method to the classical K estimator especially when small but consistent coherent components are present.

REFERENCES

1. Ferrara, G., M. Migliaccio, and A. Sorrentino, "Characterization of GSM non-line-of-sight (NLOS) propagation channels generated in a reverberating chamber by using bit-error-rates (BER)," *IEEE Trans. Electromagn. Compat.*, Vol. 49, No. 3, 467–473, 2007.
2. Sorrentino, A., G. Ferrara, and M. Migliaccio, "The reverberating chamber as emulator of radar ground clutter doppler spectra," *Proceedings of EUCAP 2010*, 1–4, Barcelona, Spain, Apr. 12–16, 2010.
3. Staniec, K., "Evaluation of the zigbee transmission repetition mechanism in the variably-loaded reverberation chamber," *Progress In Electromagnetics Research*, Vol. 132, 297–314, 2012.
4. Kostas, J. G. and B. Boverie, "Statistical model for a mode stirred chamber," *IEEE Trans. Electromagn. Compat.*, Vol. 33, No. 4, 366–370, 1991.
5. Sorrentino, A., P. S. Kildal, U. Carlberg, and E. Pucci, "Accuracy in reverberation chamber for wireless testing: Simple formulas for the number of independent samples," *Proceedings of EuCAP 2009*, 2673–2677, Berlin, Germany, Mar. 2009.
6. Sorrentino, A., L. Mascolo, G. Ferrara, and M. Migliaccio, "The fractal nature of the electromagnetic field within a reverberating chamber," *Progress In Electromagnetics Research C*, Vol. 27, 157–167, 2012.
7. Corona, P., G. Ferrara, and M. Migliaccio, "Reverberating chamber field in presence of an unstirred component," *IEEE Trans. Electromagn. Compat.*, Vol. 42, No. 2, 111–115, 2000.
8. Mariani, P. V. and F. Moglie, "Numerical simulation of LOS and NLOS conditions for an antenna inside a reverberation chamber," *Journal of Electromagnetic Waves and Applications*, Vol. 24, Nos. 17–18, 2319–2331, 2010.
9. Sorrentino, A., G. Ferrara, A. Gifuni, and M. Migliaccio, "Antenna pattern in a multipath environment emulated in a

reverberating chamber," *Proceedings of EUCAP 2013*, 3561–3165, Gothenburg, Sweden, Apr. 8–12, 2013.

10. Khaleghi, A., "Diversity techniques with parallel dipole antennas: Radiation pattern analysis," *Progress In Electromagnetics Research*, Vol. 64, 23–42, 2006.
11. Ferrara, G., A. Gifuni, and A. Sorrentino, "Test on antennas in a reverberating chamber and comparison with anechoic chamber," *Proceedings of EUCAP 2012*, 2154–2157, Prague, Czech Republic, Mar. 26–30, 2012.
12. Chen, X., "Measurements and evaluations of multi-element antennas based on limited channel samples in a reverberation chamber," *Progress In Electromagnetics Research*, Vol. 131, 45–62, 2012.
13. Sorrentino, A., F. Nunziata, G. Ferrara, and M. Migliaccio, "Reverberating chamber profile identification," *IET Microwaves, Antennas & Propagation*, Vol. 6, No. 13, 1468–1472, 2012.
14. Sorrentino, A., G. Ferrara, and M. Migliaccio, "The kurtosis index to characterize near LOS conditions in reverberating chambers," *IET Microwave, Antennas & Propagation*, Vol. 7, No. 3, 175–179, 2013.
15. Sorrentino, A., G. Ferrara, and M. Migliaccio, "On the coherence time control of a continuous mode stirred reverberating chamber," *IEEE Trans. on Antennas and Propagation*, Vol. 57, No. 10, 3372–3374, 2009.
16. Sorrentino, A., G. Ferrara, and M. Migliaccio, "The reverberating chamber as a line-of-sight wireless channel emulator," *IEEE Trans. on Antennas and Propagation*, Vol. 56, No. 6, 1825–1830, 2008.
17. Holloway, C. L., D. A. Hill, J. M. Ladbury, P. F. Wilson, G. Koepke, and J. Coder, "On the use of reverberation chambers to simulate a Rician radio environment for the testing of wireless devices," *IEEE Trans. on Antennas and Propagation*, Vol. 54, No. 11, 1–11, 2006.
18. Sorrentino, A., G. Ferrara, and M. Migliaccio, "An effective indicator for NLOS, nLOS, LOS propagation channels conditions," *Proceedings of EUCAP 2012*, 1422–1426, Mar. 26–30, 2012.
19. Kildal, P. S. and K. Rosengren, "Correlation and capacity of MIMO systems and mutual coupling, radiation efficiency and diversity gain of their antennas: Simulations and measurements in reverberation chamber," *IEEE Communications Magazine*, Vol. 42, No. 12, 102–112, 2004.

20. Chen, X., P. S. Kildal, J. Carlsson, and J. Yang, "Comparison of ergodic capacities from wideband MIMO antenna measurements in reverberation chamber and anechoic chamber," *IEEE Antennas and Wireless Propagation Letters*, Vol. 10, 466–469, 2011.
21. Lemoine, C., E. Amador, and P. Besnier, "On the K-factor estimation for Rician channel simulated in reverberation chamber," *IEEE Trans. on Antennas and Propagation*, Vol. 59, No. 3, 1003–1012, 2011.
22. Lemoine, C., P. Besnier, and M. Drissi, "Advanced method for estimating direct-to-scattered ratio of Rician channel in a reverberation chamber," *Electron. Lett.*, Vol. 45, No. 4, 194–196, 2009.
23. Ionut, M., P. Besnier, and C. Lemoine, "Estimating the K-factor and time spread parameters from a transient response of a pulse modulated sine wave in reverberation chamber," *IEEE Trans. on Antennas and Propagation*, Vol. 61, No. 1, 380–389, 2013.
24. Tepedelenlioglu, C., A. Abdi, and G. B. Giannakis, "The Ricean K factor: Estimation and performance analysis," *IEEE Trans. Wireless Commun.*, Vol. 2, No. 4, 799–810, 2003.
25. Baddour, K. E. and T. J. Willink, "Improved estimation of the Ricean K-factor from I/Q fading channel samples," *IEEE Trans. Wireless Commun.*, Vol. 7, No. 12, 5051–5057, 2008.
26. Ren, J. and R. G. Vaughan, "Rice factor estimation from the channel phase," *IEEE Trans. Wireless Commun.*, Vol. 11, No. 6, 1976–1980, 2012.
27. Valenzuela-Valdés, J. F., A. M. Martìnez-Gonzaléz, and D. A. Sànchez-Hernàndez, "Emulation of MIMO nonisotropic fading environments with reverberation chambers," *IEEE Trans. on Antenna and Wirelles Propag. Letters*, Vol. 7, 325–328, 2008.
28. Papoulis, A., *Probability, Random Variables and Stochastic Process,* MacGraw-Hill, New York, 1991.
29. Moglie, F. and V. M. Primiani, "Numerical analysis of a new location for the working volume inside a reverberation chamber," *IEEE Trans. Electromagn. Compat.*, Vol. 54, No. 2, 238–245, 2012.